

Probing the Strong Boundary Shape Dependence of the Casimir Force

Thorsten Emig¹, Andreas Hanke¹, Ramin Golestanian^{2,4}, Mehran Kardar^{1,3}

¹*Physics Department, Massachusetts Institute of Technology, Cambridge, MA 02139*

²*Institute for Advanced Studies in Basic Sciences, Zanjan 45195-159, Iran*

³*Institute for Theoretical Physics, University of California, Santa Barbara, CA 93106*

⁴*Institute for Studies in Theoretical Physics and Mathematics, P.O. Box 19395-5531, Tehran, Iran*

(October 30, 2018)

We study the geometry dependence of the Casimir energy for deformed metal plates by a path integral quantization of the electromagnetic field. For the first time, we give a complete analytical result for the deformation induced change in Casimir energy $\delta\mathcal{E}$ in an experimentally testable, nontrivial geometry, consisting of a flat and a corrugated plate. Our results show an interesting crossover for $\delta\mathcal{E}$ as a function of the ratio of the mean plate distance H , to the corrugation length λ : For $\lambda \ll H$ we find a *slower* decay $\sim H^{-4}$, compared to the H^{-5} behavior predicted by the commonly used pairwise summation of van der Waals forces, which is valid only for $\lambda \gg H$.

PACS numbers: 03.70.+k, 11.10.-z, 42.50.Ct, 12.20.-m

In 1948, Casimir showed that two parallel conducting plates, separated by a distance H , attract each other with a force F , proportional to the surface area A , and given by [1]

$$\frac{F}{A} = -\frac{\pi^2}{240} \frac{\hbar c}{H^4}. \quad (1)$$

This remarkable prediction of quantum electrodynamics can be understood as resulting from the modification of the zero point vacuum fluctuations of the electromagnetic field by the presence of boundaries. Since this discovery, the fundamental nature of the Casimir effect and its implications, e.g., on surface forces [2], particle physics [3], and cosmology [4], has motivated extensive theoretical work (see Refs. [5–9] for reviews). On the experimental front, the initial attempt at observing the Casimir force, by Sparnaay in 1958, was not conclusive due to large experimental uncertainty [10]. Only recently, there have been a number of precision measurements of the Casimir force, using a torsion pendulum [11], an atomic force microscope [12], and a micromachined torsional device [13], which confirm the theory to a few per cent accuracy. The latter experiment also demonstrates the possibility for novel actuation schemes in microelectromechanical systems based on the Casimir force [14].

In the more general context of the Lifshitz theory for dielectric bodies [15], Eq. (1) appears in the limit of perfectly conducting plates, for which the dielectric constant ε is infinite. For finite $\varepsilon = \varepsilon(\omega)$, this power law for the force is recovered for large distances $H \gg c/\omega_0$, where ω_0 is the smallest resonance (absorption) frequency of the dielectric (usually $c/\omega_0 \approx 10\text{--}100$ nm). In this, so-called retarded, limit, the force is *universal* in the sense that it only depends on the electrostatic dielectric constant $\varepsilon_0 = \varepsilon(0)$, and can be obtained, e.g., by dispersion relation techniques [16]. The opposite limit of $H \ll c/\omega_0$ gives the unretarded van der Waals force $F/A \sim H^{-3}$, which can also be obtained by summing the (attractive)

intermolecular interactions due to induced molecular dipole moments. Even though obtainable from the same microscopic theory, the Casimir and van der Waals forces are quite different. In particular, the interpretation of the Casimir force in terms of changes in zero point vacuum electromagnetic energy suggests it to be a strong function of geometry [17,18]; probing the global shape of the boundary that confines the vacuum fluctuations. Indeed, whereas the van der Waals force between electrically polarizable particles is always attractive, even the *sign* of the Casimir force is geometry dependent, and can be *repulsive*, e.g., for a thin spherical or cubic shell [6,7,17]. (Repulsive Casimir forces are expected also when *magnetic* as well as electric properties are included [16,19].)

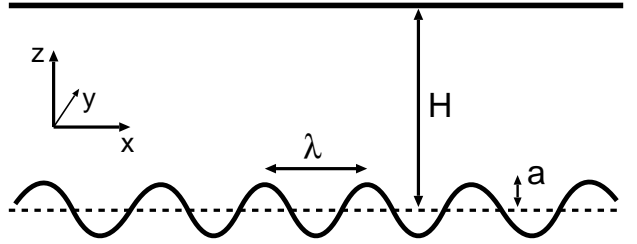


FIG. 1. Geometry used for calculating the Casimir energy of a flat plate and a corrugated plate at mean distance H .

It is highly desirable to demonstrate the strong shape dependence of the Casimir interaction in a set-up that clearly demonstrates its distinction from the usual pairwise additive interactions [20]. Since measurement of the repulsive Casimir interaction for a conducting sphere is experimentally difficult, the most promising route is to via modifications of the parallel plate geometry. In searching for nontrivial boundary dependences, Roy and Mohideen [21] examined the force between a sphere, and a sinusoidally corrugated plate with amplitude $a \approx 60$ nm and wavelength $\lambda \approx 1.1 \mu\text{m}$. Over the range of separations $H \approx 0.1 - 0.9 \mu\text{m}$, the observed force showed clear

deviations from the dependence expected on the basis of decomposing the Casimir force to a sum of pairwise contributions (in effect, an average over the variations in separations). This experimental result motivated our calculation of the exact Casimir force in the geometry depicted in Fig. 1, without the assumption of pairwise additivity. Our analytic results [see Eqs. (4) - (6) and Fig. 2] hold to second order in a , and show that for fixed H the corrections due to corrugation strongly depend on λ . In fact, for $H/\lambda \gg 1$ the correction is by a factor of H/λ larger than in the opposite limit of $H/\lambda \ll 1$ where the assumption of pairwise additivity is asymptotically correct. However, the experiments of Ref. [21] are performed in the range of $H/\lambda \approx 0.1 - 0.8$ where the corrections to pairwise additivity are in fact not significant enough to account for the observed deviations. This bolsters the conclusion in Ref. [22] that these deviations are in fact due to a lateral force that tends to preferentially position the spherical AFM tip on top of local maxima of the modulated surface (leading to a smaller separation and stronger force). We thus propose that the shape dependence of the Casimir force can in fact be probed in this set-up by going to modulations of shorter wavelength; a hard but achievable goal.

The use of a spherical tip, of large radius R , in experiments [11–13] causes some differences from the flat plate geometry used in our calculations. First, the positioning of the tip relative to the modulations is important when H and λ are comparable, but becomes insignificant in the proposed limit of $\lambda \ll H, R$. Secondly, as long as $R \gg H, \lambda$ the curvature of the tip does not lead to nontrivial corrections, and the force can be related to the energy per surface area \mathcal{E} in Eq. (5) by the proximity force rule $F = 2\pi R\mathcal{E}$ [23]. These formulae thus provide a specific recipe for evaluating the nontrivial shape dependences of the Casimir force in the experimental set-up.

Before turning to the geometry of Fig. 1, consider the more general case of two perfectly conducting plates of mean separation H , which are infinitely extended along the x - y plane. Now assume that one of the plates is deformed in a way that is translationally invariant along the y axis and has no overhangs. Its profile can then be described by the height function $h(x)$, with $\int dx h(x) = 0$. For example, to describe the geometry in the experiment of Ref. [21], we choose $h(x) = a \cos(2\pi x/\lambda)$ as in Fig. 1. The Casimir energy associated with general $h(x)$ at zero temperature corresponds to the difference of the ground state energies of the quantized electromagnetic (EM) field with and without plates, respectively. To obtain this energy, we employ the path integral quantization method, which can be applied to the EM gauge field by introducing a suitable gauge fixing procedure [24]. However, in the present translationally invariant geometry we can develop a simpler quantization scheme, by a similar reasoning as used in the context of waveguides with constant

cross-sectional shape (here along the y axis) [25]. For an arbitrary EM field between the plates, transverse components of the E and B fields are completely determined by their axial components E_y and B_y . Therefore, any EM field can be described by a superposition of two independent scalar fields $\Phi_{\text{TM}} \equiv E_y$ (transverse magnetic waves, $B_y = 0$) and $\Phi_{\text{TE}} \equiv B_y$ (transverse electric waves, $E_y = 0$). The scalar fields both fulfill the usual wave equation, but differ in their boundary conditions on the plates S , as $\Phi_{\text{TM}}|_S = 0$, while $\partial_n \Phi_{\text{TE}}|_S = 0$, where ∂_n denotes the normal derivative.

Both scalar fields can now be quantized by considering the Euclidean action $S[\Phi] = \frac{1}{2} \int d^4 X (\nabla \Phi)^2$, corresponding to the wave equation after a Wick rotation to the imaginary time $X^0 = ict$. In the 4D Euclidean space, the plates are parametrized by $X_1(\mathbf{r}) = [\mathbf{r}, h(x)]$ and $X_2(\mathbf{r}) = [\mathbf{r}, H]$, with $\mathbf{r} = (ict, x, y)$. We implement the boundary conditions on S using delta functions [20,26], leading to the partition function

$$\mathcal{Z} = \frac{1}{\mathcal{Z}_0} \int \mathcal{D}\Phi \prod_{j=1}^2 C[\Phi(X_j)] \exp(-S[\Phi]/\hbar), \quad (2)$$

with the boundary condition enforcing functionals $C[\Phi(X_j)] = \prod_{\mathbf{r}} \delta(\Phi(X_j(\mathbf{r})))$ for Φ_{TM} , and $C[\Phi(X_j)] = \prod_{\mathbf{r}} \delta(\partial_n \Phi(X_j(\mathbf{r})))$ for Φ_{TE} , and the partition function \mathcal{Z}_0 of the space without plates. The Casimir energy per surface area A is then given by $\mathcal{E} = -\hbar c \ln \mathcal{Z}/AL$ where L is the overall Euclidean length in time direction. Implementing the delta functions by integrals over auxiliary fields and integrating out Φ , we obtain an $h(x)$ dependent kernel M for the Gaussian action of the auxiliary fields. Expanding $\mathcal{Z} = (\det M)^{-1/2}$ to second order in $h(x)$, we get for the deformation dependent part of \mathcal{Z} ,

$$\ln \mathcal{Z}_h = \frac{1}{2} \int_{\mathbf{r}} \int_{\mathbf{r}'} K(\mathbf{r} - \mathbf{r}') h(x) h(x'). \quad (3)$$

The kernel is the sum of contributions from the two wave types, i.e., $K(\mathbf{r}) = K_{\text{TM}}(|\mathbf{r}|) + K_{\text{TE}}(|r_0|, |\mathbf{r}_\parallel|)$, with $\mathbf{r} = (r_0, \mathbf{r}_\parallel)$, and has been calculated explicitly.

For the specific deformation of the plates corresponding to harmonic corrugation of amplitude a and wavelength λ defined above, the calculation of $\ln \mathcal{Z}_h$ reduces to Fourier transforming the kernel $K(\mathbf{r})$. The corresponding integrals can be performed for $\lambda > 0$ by closing the integration contour via a semi-circle at infinity in the upper half of the complex plane. The resulting sum of an infinite series of residues can be expressed in terms of the polylogarithm function $\text{Li}_n(z) \equiv \sum_{\nu=1}^{\infty} z^\nu / \nu^n$, leading to

$$\mathcal{E} = -\frac{\hbar c}{H^3} \left\{ \frac{\pi^2}{720} + \frac{a^2}{H^2} \left[G_{\text{TM}} \left(\frac{H}{\lambda} \right) + G_{\text{TE}} \left(\frac{H}{\lambda} \right) \right] \right\}. \quad (4)$$

The contributions from TM and TE modes are:

$$G_{\text{TM}}(s) = \frac{\pi^3 s}{480} - \frac{\pi^2 s^4}{30} \ln(1-u) + \frac{\pi}{1920s} \text{Li}_2(1-u) + \frac{\pi s^3}{24} \text{Li}_2(u) + \frac{s^2}{24} \text{Li}_3(u) + \frac{s}{32\pi} \text{Li}_4(u) + \frac{1}{64\pi^2} \text{Li}_5(u) + \frac{1}{256\pi^3 s} \left(\text{Li}_6(u) - \frac{\pi^6}{945} \right), \quad (5)$$

$$G_{\text{TE}}(s) = \frac{\pi^3 s}{1440} - \frac{\pi^2 s^4}{30} \ln(1-u) + \frac{\pi}{1920s} \text{Li}_2(1-u) - \frac{\pi s}{48} (1+2s^2) \text{Li}_2(u) + \left(\frac{s^2}{48} - \frac{1}{64} \right) \text{Li}_3(u) + \frac{5s}{64\pi} \text{Li}_4(u) + \frac{7}{128\pi^2} \text{Li}_5(u) + \frac{1}{256\pi^3 s} \left(\frac{7}{2} \text{Li}_6(u) - \pi^2 \text{Li}_4(u) + \frac{\pi^6}{135} \right), \quad (6)$$

with $u \equiv \exp(-4\pi s)$. Figure 2 displays separately the contributions from G_{TM} and G_{TE} to the corrugation induced correction $\delta\mathcal{E}$ to the Casimir energy. While $G_{\text{TM}}(H/\lambda)$ is a monotonically increasing function of H/λ , $G_{\text{TE}}(H/\lambda)$ displays a minimum for $H/\lambda \approx 0.3$. The net Casimir energy \mathcal{E} is shown in Fig. 3 for two representative values of a/λ , including the parameters used in the experiment of Ref. [21]. Note that the corrugation induced correction leads to a larger energy \mathcal{E} , and hence the corresponding force $F = 2\pi R\mathcal{E}$ is *enhanced*.

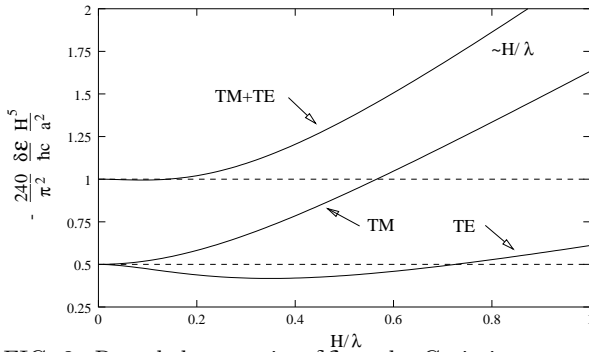


FIG. 2. Rescaled correction $\delta\mathcal{E}$ to the Casimir energy due to the corrugation as given by the terms in square brackets of Eq. (4) (upper curve). The lower curves show the separate contributions from TM and TE modes. The rescaling of $\delta\mathcal{E}$ is chosen such that the result from a pairwise summation of van der Waals forces is a constant (dashed lines).

Examining the limiting behaviors of Eq. (4) is instructive. In the limit $\lambda \gg H$, the functions G_{TM} and G_{TE} approach constant values, and the Casimir energy takes the λ -independent form

$$\mathcal{E} = -\frac{\hbar c}{H^3} \frac{\pi^2}{720} \left(1 + 3 \frac{a^2}{H^2} \right). \quad (7)$$

Note that only in this case both wave types provide the same contribution to the total energy, see Fig. 2. In the opposite limit of $\lambda \ll H$, as suggested by the first terms in Eqs. (5), (6), both G_{TM} and G_{TE} grow linearly in H/λ . Therefore, in this limit the correction to the Casimir energy decays *slower*, according to a new power law in H ,

$$\mathcal{E} = -\frac{\hbar c}{H^3} \frac{\pi^2}{720} \left(1 + 2\pi \frac{a^2}{\lambda H} \right), \quad (8)$$

with an amplitude proportional to $1/\lambda$. Analyzing the correction $\delta\mathcal{E}$ in the limit $a, \lambda \ll H$ for *arbitrary* values of a/λ , we find that the factor multiplying a/H in Eq. (8) saturates for $\lambda \ll a$ at a number of order unity. This result can be justified by noting that the most relevant contributions to the force come from modes of wavelength of order H . The corrugation also affects modes of wavelength of order λ , but these modes contribute to the single plate energy only. Thus, in the extreme limit $\lambda \ll a$, one has a clear separation of the length scales H and λ , and the modes “see” flat plates at an effective separation $H - a$, leading to a correction of the order a/H after expansion in a .

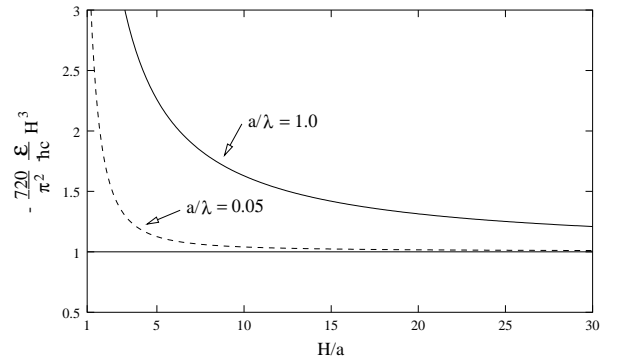


FIG. 3. Rescaled Casimir energy as given by Eq. (4) for two fixed values of a/λ . The rescaling is chosen such that the Casimir energy of two flat plates becomes one (horizontal line). The lower curve with $a/\lambda = 0.05$ corresponds to the parameters used in the experiment of Ref. [21], where H/a varies between approximately 3 and 17.

The above behavior of the correction $\delta\mathcal{E}$ for small and large H/λ clarifies the limits of validity of previous results in the literature. The upper dashed line in Fig. 2 corresponds to a widely used approach [2,27] in which the interaction is obtained from a pairwise summation of ‘van der Waals type’ two body forces. It is evident that this approximation is accurate only for $H/\lambda \rightarrow 0$, which in this limit is equivalent to the Derjaguin method to any order in the amplitude a [23]. Already for H/λ of order unity, the additive van der Waals type approximation breaks down. The opposite limit, $H/\lambda \rightarrow \infty$, corroborates the result reported in Ref. [28], which is larger than the former by a factor of $H/\lambda \gg 1$. However, in experi-

ments with lateral distortions λ of the order of H , none of the above limiting cases is realized, which makes the present, more complete analysis necessary.

Moreover, for purposes of experimental comparison, corrections due to finite conductivity of the plates, surface roughness, and finite temperature should be taken into account. These corrections introduce additional length scales into the problem, which are in turn the plasma wavelength λ_p of the plates (e.g., $\lambda_p \approx 100$ nm for aluminium [12,21]), the transverse correlation length ξ of the roughness (usually $\xi \approx 300$ nm [13]), and the thermal wavelength $\lambda_T = \hbar c/k_B T$ ($\approx 1 \mu\text{m}$ at 300°K). The plasma and thermal wavelengths provide lower and upper bounds for H , respectively, such that our results for perfectly conducting plates at zero temperature are valid for $\lambda, H \gg \lambda_p$, and $H \ll \lambda_T$ [29].

Finally, we note that in the set-up of Fig. 1 nontrivial shape dependencies appear as corrections to a larger Casimir force. For the purpose of experimental tests, it is much more desirable to devise set-ups which directly probe differences, without the need for subtracting a larger baseline force. For example, in an atomic force experiment, simultaneous scanning of a flat and corrugated substrate would be desirable; while in the torsion pendulum experiment, one can imagine suspending a spherical lens equidistantly from two plates, one of which is corrugated. Another potential experiment along these lines is to measure the lateral force between two plates with sinusoidal corrugations of the same wavelength λ , which are shifted relative to each other by a distance δ . We find a lateral force $F_{\parallel} = \hbar c \frac{a^2}{\lambda H^3} \sin(2\pi\delta/\lambda) g(H/\lambda)$. This force tends to change the position of the plates such that a maximum is opposite to a minimum, corresponding to $\delta = \lambda/2$. The universal function $g(H/\lambda)$ tends to a finite value for $H/\lambda \rightarrow 0$, but vanishes exponentially for large H/λ . Similar results hold for the alternating component of the standard Casimir force as a function of the phase shift between the plates.

We thank J.-P. Bouchaud, S. Dietrich, S. G. Johnson, M. L. Povinelli, and S. Scheidl for useful discussions. This work was supported by the Deutsche Forschungsgemeinschaft under grants No. EM70/1-3 (T.E.), HA3030/1-2 (A.H.), and the National Science Foundation through grants No. DMR-01-18213, and PHY99-07949 (M.K.).

[1] H. B. G. Casimir, Proc. K. Ned. Akad. Wet. **51**, 793 (1948).
 [2] J. N. Israelachvili, *Intermolecular and Surface Forces* (Academic, London, 1992).
 [3] K. A. Milton, Phys. Rev. D **22**, 1441; **22**, 1444 (1980).
 [4] I. Brevik and H. Kolbenstvedt, Nuovo Cimento B **82**, 71 (1984).
 [5] G. Plunien, B. Müller, and W. Greiner, Phys. Rep. **134**, 87 (1986).

[6] V. M. Mostepanenko and N. N. Trunov, *The Casimir Effect and its Applications* (Clarendon, Oxford, 1997).
 [7] E. Elizalde and A. Romeo, Am. J. Phys. **59**, 711 (1991).
 [8] P. W. Milonni, *The Quantum Vacuum* (Academic, San Diego, 1994).
 [9] M. Kardar and R. Golestanian, Rev. Mod. Phys. **71**, 1233 (1999).
 [10] M. J. Sparnaay, Physica (Utrecht) **24**, 751 (1958).
 [11] S. K. Lamoreaux, Phys. Rev. Lett. **78**, 5 (1997); **81**, 5475(E) (1998).
 [12] U. Mohideen and A. Roy, Phys. Rev. Lett. **81**, 4549 (1998).
 [13] H. B. Chan, V. A. Aksyuk, R. N. Kleiman, D. J. Bishop, and F. Capasso, Science **291**, 1941 (2001).
 [14] F. M. Serry, D. Walliser, and G. J. Maclay, J. Microelectromech. Syst. **4**, 193 (1995).
 [15] E. M. Lifshitz, Sov. Phys. JETP **2**, 73 (1956); I. E. Dzyaloshinskii, E. M. Lifshitz, and L. P. Pitaevskii, Adv. Phys. **10**, 165 (1961).
 [16] G. Feinberg and J. Sucher, Phys. Rev. A **2**, 2395 (1970).
 [17] R. Balian and B. Duplantier, Ann. Phys. (New York) **104**, 300 (1977); **112**, 165 (1978).
 [18] However, one should note that by virtue of Schwinger's source theory [J. Schwinger, L. L. DeRaad, Jr., and K. A. Milton, Ann. Phys. (New York) **115**, 1 (1978)], the Casimir force can be obtained without referring to vacuum fluctuations; see also Ref. [8].
 [19] T. Boyer, Phys. Rev. A **9**, 2078 (1974); V. Hushwater, Am. J. Phys. **65**, 381 (1997).
 [20] R. Golestanian and M. Kardar, Phys. Rev. Lett. **78**, 3421 (1997); Phys. Rev. A **58**, 1713 (1998).
 [21] A. Roy and U. Mohideen, Phys. Rev. Lett. **82**, 4380 (1999).
 [22] G. L. Klimchitskaya, S. I. Zanette, and A. O. Caride, Phys. Rev. A **63**, 14101 (2000).
 [23] B. Derjaguin, Kolloid Z. **69**, 155 (1934).
 [24] M. E. Peskin, and D. V. Schroeder, *An Introduction to Quantum Field Theory* (Addison-Wesley, Reading, 1995).
 [25] J. D. Jackson, *Classical Electrodynamics* (Wiley, New York, 1999).
 [26] Following the introduction of the path integral method, further applications have been considered in O. Kenneth and S. Nussinov, Phys. Rev. D **63**, 121701 (2001); for a single corrugated plate, see also A. Hanke and M. Kardar, Phys. Rev. Lett. **86**, 4596 (2001).
 [27] M. Bordag, G. L. Klimchitskaya, and V. M. Mostepanenko, Mod. Phys. Lett. A **9**, 2515 (1994); Int. J. Mod. Phys. A **10**, 2661 (1995).
 [28] S. K. Karepanov, M. Y. Novikov, and A. S. Sorin, Nuovo Cimento B **100**, 411 (1987).
 [29] The importance of stochastic surface roughness can also be deduced from our calculations. The relative corrections $\delta\mathcal{E}/\mathcal{E}$ to the Casimir energy due to roughness of amplitude a and transverse correlation length ξ should be of the form a^2/H^2 for $\xi \gg H$, and $a^2/(\xi H)$ for $\xi \ll H$. While the latter behavior is in accordance with Ref. [30], we note that the experimental case corresponds to neither extreme, making a more complete analysis necessary.
 [30] M. Y. Novikov, A. S. Sorin, and V. Y. Chernyak, Theor. Math. Phys. **82**, 124 (1990); **82**, 252 (1990); **91**, 658 (1992); **92**, 773 (1992).